Optimizing Material Composition in Aircraft Wing Design for Reduced Lifecycle Environmental Impact

Cobo-Urios Almudena, Silva-Vilela-Caridade Álvaro
Supervisor: Joseph Morlier
S2 Final Report

June 24, 2025

Abstract

This project investigates the role of composite materials in improving the structural and environmental performance of aircraft wings, with a focus on their aeroelastic behavior. Using the OpenAeroStruct tool, we optimise wing structures for different materials, such as aluminium, CFRP, titanium, and steel, while considering constraints related to stress, buckling, and range. We then extend the material selection process using a Variational Autoencoder (VAE), which enables the continuous representation of discrete material databases. This approach allows for gradient-based, multi-objective optimization of mechanical and environmental trade-offs (cost, energy, waste, density, young modulus, and yield stress). Optimal material solutions are identified through the analysis of Pareto fronts, revealing hybrid, potentially non-existent materials that offer superior trade-offs across conflicting objectives. The proposed methodology integrates machine learning and design optimization to support sustainable aerospace innovation, and the selected material is later reintegrated into the OpenAeroStruct model to assess their impact on aircraft performance. This comprehensive framework bridges data-driven design with engineering constraints, offering a novel pathway for eco-efficient material selection in early-stage aircraft design.

Keywords: Aero-structural optimization, Composite materials, Variational Autoencoder, Latent Space, Multi-objective optimization, Material Selection, OpenAeroStruct, Sustainable aerospace design

Contents

List of Figures

List of Tables

Declaration of Authenticity

This assignment is entirely our own work. Quotations from literature are properly indicated with appropriate references in the text. All literature used in this piece of work is listed in the bibliography at the end. We confirm that no sources have been used other than those stated.

We understand that plagiarism (copying without appropriate citation) is a serious academic offense that may result in disciplinary action.

Date: June 24, 2025

Signature(s):

Álvaro Caridade

1 Introduction

The aerospace industry is undergoing a transformation toward sustainability, driven by environmental regulations, fuel economy goals, and the pursuit of greener technologies. In this context, the choice of structural materials plays a critical role in shaping aircraft lifecycle performance. Composite materials, with their favorable strength-to-weight ratios, offer promising benefits, but also pose challenges related to cost, manufacturability, and end-of-life impact.

This project aims to contribute to sustainable aircraft design by investigating how structural materials, both conventional and advanced, can be selected and optimized in the early stages of conceptual design. We adopt a data-driven approach that combines engineering tools (OpenAeroStruct) with machine learning (Variational Autoencoders) and multi-objective optimization to balance mechanical, environmental, and economic performance indicators.

As a case study, we focus on the Airbus A320 family, currently the most widely deployed single-aisle aircraft. Its legacy design, originating in the 1980s, still relies heavily on conventional metallic structures. As such, even incremental structural or material improvements in this platform can translate to significant environmental gains across the global fleet. Furthermore, the continued demand for this aircraft class, combined with the industry's climate targets (e.g., Paris Agreement), reinforces the importance of evaluating sustainable alternatives within this context.

2 Goal of the Project

The goal of this project is to develop a model for optimal material selection in aircraft wing design, integrating sustainability, mechanical performance, and economic cost. Using OpenAeroStruct (OAS) as the structural-aerodynamic simulation tool, we assess baseline performance for several common materials (e.g., aluminum, CFRP, steel, titanium).

To move beyond fixed material catalogs, we implement a Variational Autoencoder (VAE) to embed material properties into a continuous latent space. This allows for gradient-based, multi-objective optimization using the Multi-Gradient Descent Algorithm (MGDA). The method yields hybrid material candidates that trade off cost, energy consumption, structural efficiency, and waste. The final objective is to identify data-driven material configurations that outperform conventional ones and to evaluate their potential for real-world use via reinjection into the OAS model.

3 Project Issues

While composite materials and data-driven design offer new opportunities, several challenges arise. First, material properties are typically catalog-based and discrete, which limits the ability to perform continuous optimization. Furthermore, trade-offs between key objectives, such as reducing fuel burn, minimizing cost, and lowering environmental impact, are often conflicting and difficult to balance manually.

Additionally, existing simulation frameworks rarely integrate environmental metrics into the structural optimization process. There is also no guarantee that an "optimal" material identified computationally is physically realizable or certifiable for aviation use. These limitations highlight the need for a unified framework that connects environmental databases, optimization techniques, and engineering tools, precisely the gap this project aims to address.

4 Main Bibliography and State of the Art

4.1 Materials

The aerospace industry has progressively shifted toward advanced composites, particularly Carbon Fiber Reinforced Polymers (CFRPs), due to their exceptional strength-to-weight ratios. However, while CFRPs contribute significantly to structural efficiency and fuel savings, end-of-life disposal and recycling remain unresolved challenges that undermine their sustainability.

Existing recycling methods, such as mechanical grinding, thermal pyrolysis, and chemical solvolysis, present trade-offs between cost, energy use, and fiber quality. As noted by Vo-Dong et al. [1], mechanical processes degrade mechanical properties, while thermal techniques reduce fiber integrity, and chemical approaches, though yielding higher-quality outputs, are economically prohibitive. Despite initiatives like the Aircraft Fleet Recycling Association (AFRA) and the Airbus PAMELA project, large-scale CFRP recycling remains limited by regulatory and market constraints.

In light of these limitations, Natural Fiber Composites (NFCs) have emerged as a bio-based alternative. Materials such as ramie, hemp, flax, and sisal, when combined with polymer matrices like epoxy and PLA, have shown potential for mass reduction. According to [2], Epoxy/Ramie composites are 14% lighter than aluminum, while PLA/Ramie achieves a 12% reduction. However, reduced stiffness in NFCs presents aeroelastic challenges, including elevated flutter risk and compromised load-bearing capacity.

A comparative study by Kling et al. [3] further emphasizes this performance gap. While CFRP with an epoxy matrix yields a 4% wingbox mass reduction for a 1000 nm mission, natural-fiber composites like Phenol-NF and PLA-NF increase mass and fuel consumption. Phenol-CF offered comparable weight savings but exhibited buckling sensitivity, illustrating structural limitations in high-load scenarios.

Complementary studies have explored sandwich composites with lightweight cores. Waddar et al. [4] investigated structures employing sisal fabric/epoxy skins and syntactic foam cores, finding that treated cenospheres reduced weight by 14.61% and improved mechanical stiffness. Enhanced filler loading increased buckling loads and natural frequencies, although dynamic performance declined under axial compression.

The Eco-Compass project [5] has also contributed to sustainable composite development, focusing on bio-based and recycled fiber reinforcements for secondary structures and cabin interiors. Their hybrid approach, combining recycled carbon fibers with bio-fibers in non-woven architectures, shows promise for reducing environmental impact while maintaining mechanical reliability.

More recently, Fantuzzi et al. [6] introduced Ultra-Light Carbon-Based Composites (ULCCs), demonstrating through Finite Element Analysis (FEA) that these materials offer higher stiffness and lower density than conventional T300/Epoxy and T1000/Epoxy systems. The results suggest potential for substantial aircraft weight reduction, improved structural efficiency, and lower operational fuel consumption.

4.2 Multidisciplinary Design Optimization

Multidisciplinary Design Optimization (MDO) has become a central paradigm in aircraft design, enabling simultaneous consideration of aerodynamics, structures, propulsion, and increasingly, environmental impact. Recent work has explored diverse computational strategies to improve both performance and sustainability outcomes.

Morlier et al. [7] propose a hybrid approach that combines Variational Autoencoders (VAE) with evolutionary algorithms for material selection and structural optimization. This method integrates mechanical performance with environmental metrics such as CO_2 emissions and embodied energy, enabling efficient exploration of trade-offs through mixed-variable optimization.

The MDO workflow presented by Ghadge et al. [8] emphasizes aeroelastic considerations by iteratively coupling loads analysis, structural optimization, and stability assessment. Starting with conceptual mass models and preliminary sizing, the process uses parametric geometry tools (ModGen) and loads evaluation (MSC Nastran) to inform optimization loops. Final post-analyses, including flutter checks, validate structural integrity and aeroelastic robustness.

Kilimtzidis et al. [9] focus on high-aspect-ratio composite airframes, which offer drag reduction and improved aerodynamic efficiency. However, increased flexibility introduces significant nonlinear aeroelastic interactions. Their study highlights the challenge of balancing low-fidelity rapid evaluations and the need for high-fidelity, computationally expensive models to capture geometric and structural complexities accurately.

Environmental integration in early-phase MDO is addressed by Parolin et al. [10], who introduce the AEco tool. AEco incorporates streamlined Life Cycle Assessment (LCA) and Monte Carlo-based uncertainty quantification to evaluate different aircraft configurations. Unlike traditional performance-centric frameworks, AEco prioritizes metrics such as CO_2 emissions and resource depletion, and uses Contribution to Variance (CTV) sensitivity analysis to identify key environmental drivers in the design.

Henderson et al. [11] develop an optimization framework that targets both fuel burn and LTO NO_x emissions. Using a combination of Augmented Lagrangian Particle Swarm Optimization (ALPSO) for single-objective problems and Genetic Algorithms (GA) for multi-objective trade-offs, the study reveals divergent design trends: low-emission aircraft tend toward low-thrust, low-pressure-ratio engines, while fuel-optimized configurations favor high-bypass-ratio engines and slender wings. The framework also examines large aircraft optimized for short-range routes, demonstrating potential efficiency gains in terms of fuel burn per passenger-kilometer.

Finally, Liu et al. [12] extend traditional single-mission design toward multi-mission optimization through an eXtended Design Structure Matrix (XDSM). Their approach couples MDA with hybrid mission analysis, leveraging high-fidelity simulation during dynamic phases and the Bréguet range equation for cruise. Optimizing reference thrust and wing area, the framework incorporates real-world mission data and linear scalarization weighting to ensure both design realism and computational efficiency.

Collectively, these works reflect a clear trend toward integrated, sustainability-aware MDO strategies. The incorporation of advanced optimization algorithms, high-fidelity modeling, and environmental metrics represents a promising path for next-generation aircraft design.

5 OpenAeroStruct Implementation

5.1 Model configuration

When modifying the structural characteristics of the wing, it is essential to consider aerodynamic-structural coupling, as these changes directly influence the aircraft's aerodynamic behavior. As part of this project, OpenAeroStruct (OAS) - a low-fidelity, open-source tool - was selected as the primary computational tool for aerodynamic and structural optimization. Over the past months, we have studied its documentation [13], analyzed example cases, and conducted trial runs to familiarize ourselves with its capabilities. Additionally, we engaged in discussions with PhD candidate Ousmane Sy to gain deeper insights into the software's application.

To apply OpenAeroStruct in a practical scenario, we were tasked with seting up the optimization model for the Airbus A321-200 and A320-200. This required searching the relevant aircraft parameters, making estimations where data was unavailable, and using the Vortex Lattice Method (VLM) mesh code for accurate wing mesh generation. The wing configuration was inspired by the CERAS model, from [14]. These modifications enabled us to conduct a complete aerodynamic and structural optimization.

Wing Geometry. We implemented a custom mesh for the A320 wing based on CERAS planform geometry. The wing was modeled as a three-section trapezoidal planform (inboard, midboard, outboard) with the following characteristics:

Parameter	**Value**
Half-span	16.955 m
Root chord	6.000 m
Kink chord 1	6.000 m
Kink chord 2	3.773 m
Tip chord	1.515 m
LE sweep (inboard)	0°
LE sweep (midboard/outboard)	27°
Twist distribution	$[6.0, 7.0, 7.0, 7.0]^\circ$
Spar thickness (control points)	[0.004, 0.004, 0.004, 0.004] m
Skin thickness (control points)	[0.003, 0.006, 0.010, 0.012] m
t/c control points	[0.1, 0.1, 0.15, 0.15]
Airfoil used	SC2-0612 (10% to 60% section)

Table 1: Main wing geometry parameters implemented in OpenAeroStruct

This mesh was generated using a custom function that linearly distributes mesh nodes across each spanwise section. A constant airfoil section was used along the span, and the structural model was implemented using the `wingbox` option in OpenAeroStruct.

Flight Profile. The optimization considers two mission segments, representing cruise and maneuver conditions:

Variable	Cruise	Maneuver
Mach number	0.78	0.58
Altitude air density [kg/m^3]	0.348	1.225
Velocity [m/s]	230.18	197.37
Load factor	1.0	2.5

Table 2: Flight profile parameters for the two mission segments

We used OpenAeroStruct's multi-point analysis framework, with `AS_point_0` representing cruise and `AS_point_1` representing the maneuver condition. These configurations include both aerodynamic and structural constraints, such as lift-equals-weight and stress failure criteria, ensuring realistic performance evaluation across the flight envelope.

Overall, the implemented setup enables full aerodynamic-structural coupling through the use of custom mesh geometry, realistic material models, and mission profiles. It lays a robust foundation for evaluating design sensitivities and optimizing wing structural layout with respect to performance and manufacturing metrics.

5.2 First Results

Material	A320		A321		Units
	Fuel Burn	Wingbox Mass	Fuel Burn	Wingbox Mass	
Al	11,233.45	4,316.62	11,984.69	5,299.17	kg
CFRP	10,358.77	1,649.44	11,345.22	1,683.10	kg
Ti	10,932.21	3,604.41	11,933.59	4,383.65	kg
Steel	13,873.20	11,571.71	15,531.61	16,218.50	kg

Table 3: Results of the Optimization for A320 and A321

The resulting performance from OAS runs for both the A320 and A321 are presented in Figure 1. It compares the fuel burn and wingbox mass for each material, highlighting the trade-offs between weight savings and structural efficiency. CFRP offers the lightest structure and lowest fuel burn, while steel results in a heavy structure and correspondingly high fuel consumption.

To further evaluate environmental and economic impacts, Figure 2 shows the total energy consumption, cost, and waste associated with the manufacturing of each wingbox per material (for A320). This analysis reveals that while CFRP provides significant performance benefits, it also involves high energy and monetary costs. Aluminum presents a more balanced trade-off, whereas steel is environmentally and structurally unfavorable in this context.

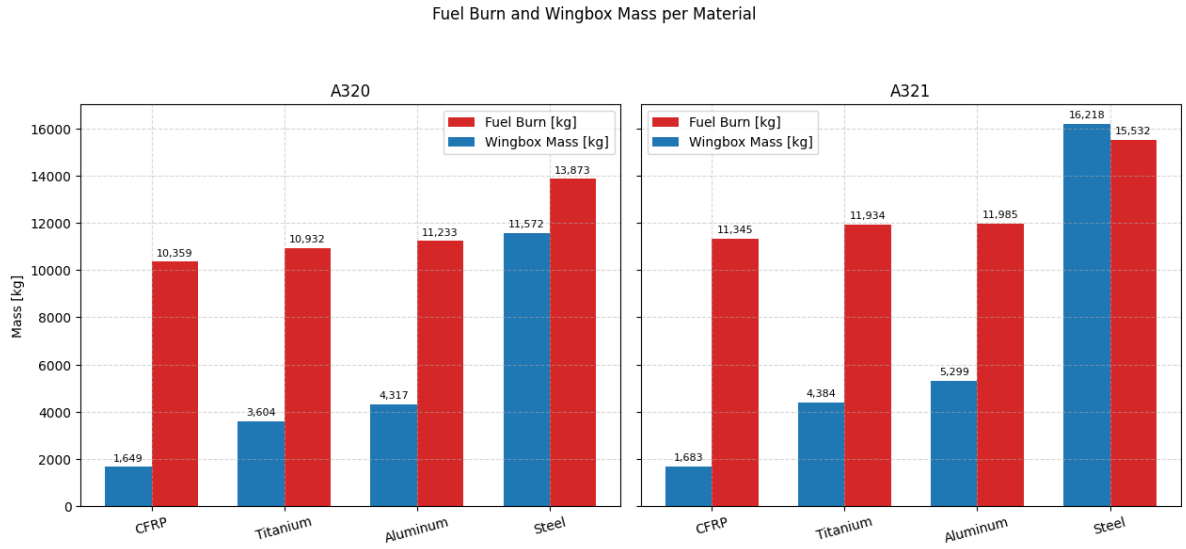

Figure 1: Fuel burn and wingbox mass per material for A320 and A321.

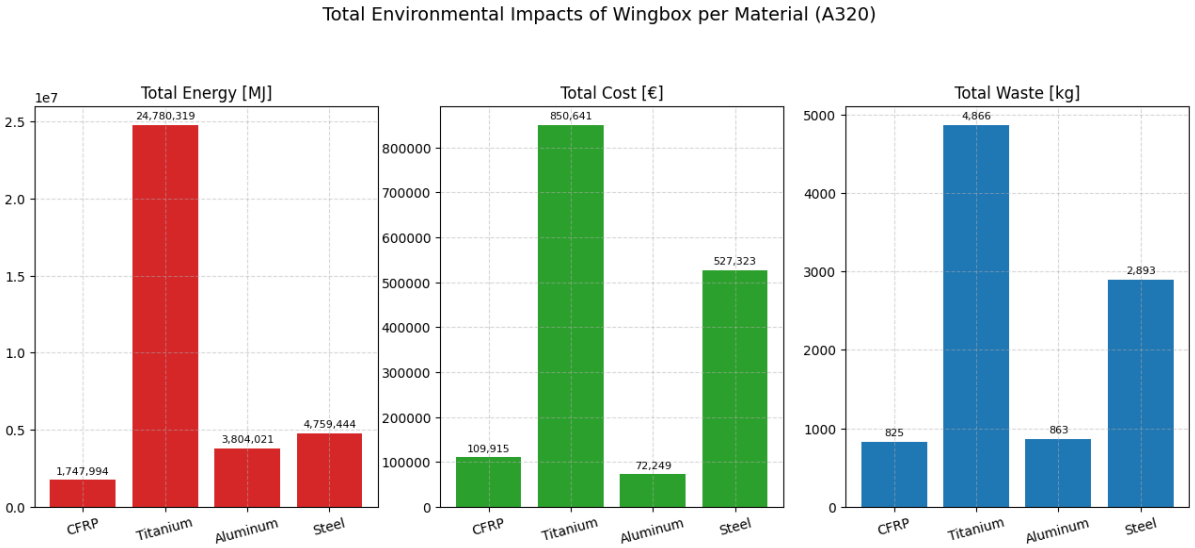

Figure 2: Total energy, cost, and waste per material for A320.

To validate the consistency of our findings, the same analysis was applied to the A321 variant (see Annex B).

Figure 3 provides a comprehensive visualization of the optimized A320 wingbox (made of CFRP), as generated by OpenAeroStruct. This figure is of particular interest for aero-structural analysis, as it presents the optimized wing geometry alongside key performance metrics, including total mass and fuel burn, as well as spatial distributions of lift, twist, thickness-to-chord ratio, structural thickness, and von Mises stress.

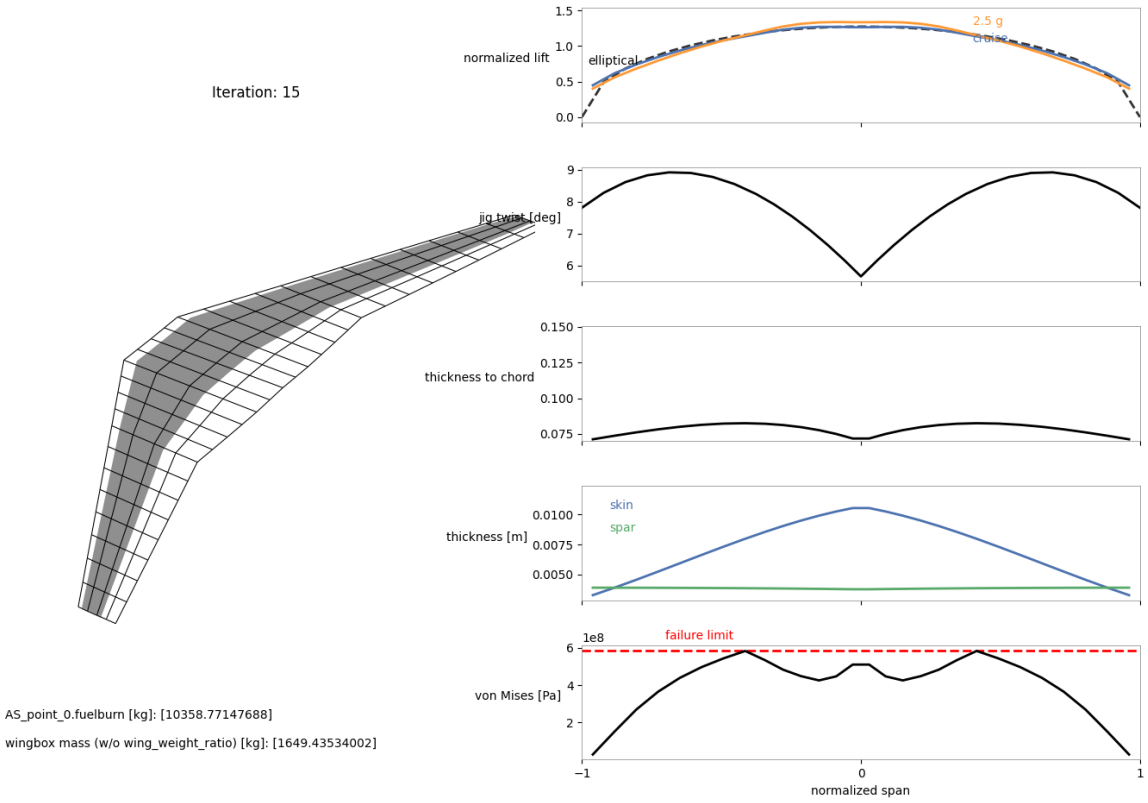

Figure 3: OpenAerostruct optimization output for A320 with CFRP wingbox

These results represent our initial optimization runs using OpenAeroStruct, performed individually for each pure material: Aluminum, Titanium, Steel, and CFRP. For each case, fuel burn was minimized while estimating the corresponding wingbox mass. These configurations serve as our baseline solutions, providing a reference point for assessing material-driven performance trade-offs. Moving forward, we aim to improve upon these results by exploring advanced material combinations and data-driven design strategies.

6 Variational Autoencoders Implementation

6.1 Overview

A *Variational Autoencoder* (VAE), first introduced in [15], is a generative neural network architecture that learns to compress high-dimensional data into a low-dimensional, continuous, and differentiable *latent space*, from which it reconstructs the original input. Unlike traditional autoencoders, VAEs introduce probabilistic inference, allowing for generalization, interpolation, and sampling from the latent space.

In this work, VAEs are used to embed discrete material data into a continuous space, enabling gradient-based optimization for material selection - an otherwise challenging task due to the categorical nature of material databases. This implementation builds upon the methodology proposed in [7], from which portions of the original codebase were adapted to fit our optimization workflow for sustainable material selection. This demonstrates the benefits of combining VAEs with evolutionary optimization for eco-design applications.

6.2 Architecture

The VAE consists of two main components:

Encoder Network: The encoder receives a normalized vector of material properties:

$$\boldsymbol{\zeta} = [C, \rho, r, \sigma_y, V, W]$$

where:

Property	**Symbol**	**Unit**
Cost per unit mass	C	€/kg
Density	ρ	kg/m^3
Density-to-stiffness ratio	r	kg/(m$^3\cdot$ GPa)
Yield stress	σ_y	MPa
Energy consumption per unit mass	V	MJ/kg
Waste generation	W	kg/kg

Table 4: Material properties with corresponding symbols and units.

It outputs:

$$\boldsymbol{\mu} = [\mu_0, \mu_1], \quad \boldsymbol{\sigma}^2 = [\sigma_0^2, \sigma_1^2]$$

Using the *reparameterization trick*, a sample is drawn from the latent space:

$$\boldsymbol{z} = \boldsymbol{\mu} + \boldsymbol{\sigma} \cdot \boldsymbol{\epsilon}, \quad \boldsymbol{\epsilon} \sim \mathcal{N}(0, I)$$

Decoder Network The decoder maps the latent vector $\boldsymbol{z} = [z_0, z_1]$ back to the estimated material properties:

$$\hat{\boldsymbol{\zeta}} = [\hat{C}, \hat{\rho}, \hat{r}, \hat{\sigma}_y, \hat{V}, \hat{W}]$$

6.3 Loss Function

The training minimizes the following objective:

$$\mathcal{L} = \|\hat{\boldsymbol{\zeta}} - \boldsymbol{\zeta}\|^2 + \beta \cdot \mathrm{KL}\left(\mathcal{N}(\boldsymbol{\mu}, \boldsymbol{\sigma}^2) \parallel \mathcal{N}(0, I)\right) \tag{1}$$

where:

- The first term is the reconstruction loss (MSE)
- The second term is the Kullback–Leibler divergence
- β is a weighting coefficient (e.g., $\beta = 5 \times 10^{-5}$)

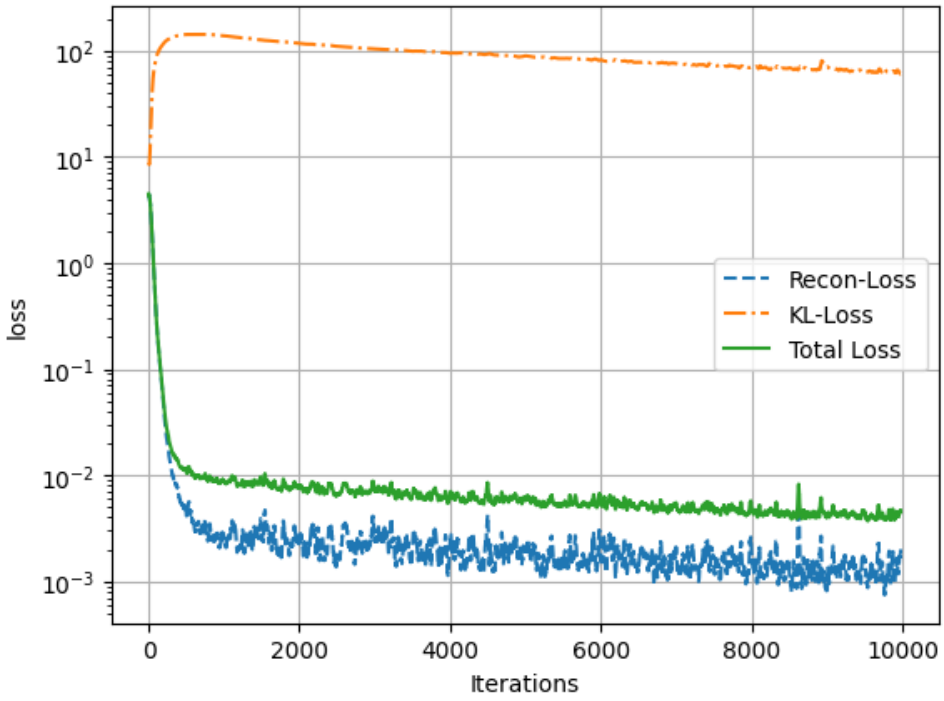

Figure 4: VAE training loss as a function of iterations.

6.4 Training Setup

- Framework: PyTorch [16]
- Network architecture: Fully connected with 250 neurons in encoder and decoder
- Latent space: 2D (z_0, z_1)
- Inputs normalized to [0, 1]; outputs rescaled post-decoding
- Training time: 3 minutes on a CPU (50,000 iterations)

6.5 Benefits for Material Selection

VAEs enable:

- **Differentiable optimization**: Gradients of decoded properties w.r.t. latent variables

$$\frac{\partial \hat{E}}{\partial z_0}, \quad \frac{\partial \hat{C}}{\partial z_1}, \quad \text{etc.}$$

- **Interpolation**: New combinations of materials with hybrid properties
- **Dimensionality reduction**: Simplifies optimization over material properties

6.6 Material Database

The seven materials selected for this study were Aluminum 2024, Aluminum 6061, CFRP Unidirectional, CFRP Woven, GFRP, Titanium, and Steel. They represent the most commonly used structural materials in aircraft wings. This selection was guided by findings in [17], which identifies these as the most representative in aerospace wing applications.

To ensure consistency in material properties across design and environmental metrics, we used data obtained from the Granta EduPack materials database [18]. Table 5 summarizes the relevant physical, economic, and environmental properties used in our optimization and latent space embedding models.

Property	**Al 2024**	**Al 6061**	**CFRP-UD**	**CFRP-Woven**	**GFRP**	**Titanium**	**Steel**
ρ [kg/m^3]	2765	2710	1565	1575	1850	4430	7740
Cost [€/kg]	17.28	16.20	55.28	78.00	76.80	236.00	45.57
Energy [MJ/kg]	872.5	890.0	1091.3	1091.3	311.7	6875.0	411.3
Waste [kg/kg]	0.20	0.20	0.50	0.50	2.00	1.35	0.25
E [GPa]	73.85	68.30	141.50	65.70	33.30	114.50	200.00
σ_y [MPa]	331.0	127.5	1955.0	768.5	368.5	848.0	698.5

Table 5: Material properties used in this study, based on Granta EduPack [18].

6.7 Implementation

The learned 2D latent space provides a continuous, low-dimensional representation of material properties, enabling smooth interpolation between known material classes. To qualitatively assess the structure of this latent space, we plot the locations of the 7 pure materials used during training (Al 2024, Al 6061, CFRP UD, CFRP Woven, GFRP, Titanium, Steel) in Figure 5.

To further understand how physical and environmental properties are distributed across the latent space, we visualize six contour maps, each corresponding to one decoded property: cost (C), density (ρ), density-to-stiffness ratio (r), yield stress (Y), energy consumption (V), and waste generation (W). These maps, provided in Appendix A, illustrate the non-linear trade-offs captured by the decoder and guide the material optimization process by indicating gradients of increasing or decreasing property values.

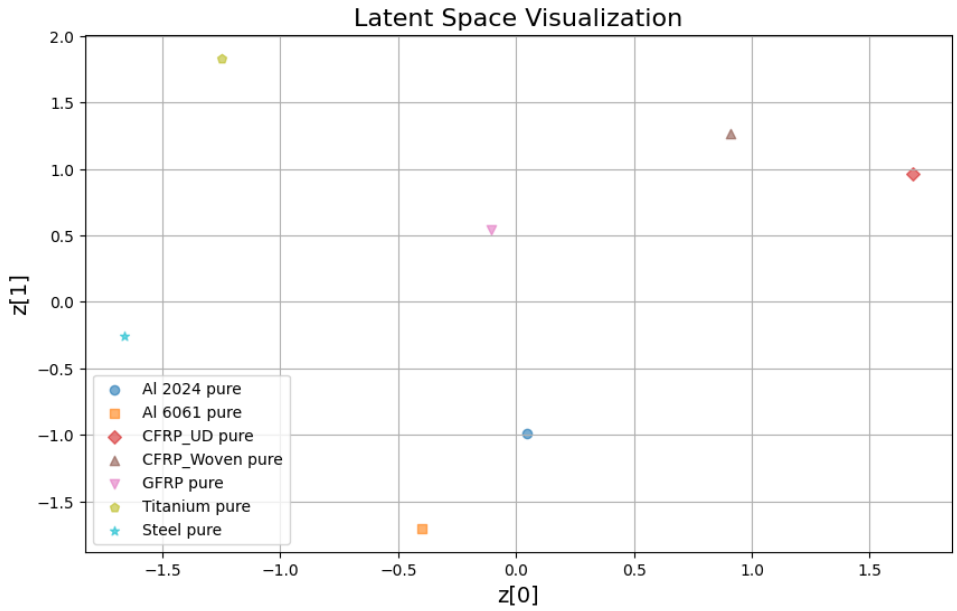

Figure 5: 2D latent space learned by the VAE colored by material class.

6.8 Post-VAE Optimization

Following the training of the VAE, we will conduct a *multi-objective optimization* procedure directly within the learned latent space. This optimization uses the gradient information obtained from the decoder network to efficiently identify optimal latent vectors.

7 Multi-Objective Optimization

The material selection problem is inherently multi-objective: improving one property (e.g., stiffness) often leads to the deterioration of another (e.g., density or environmental impact). To effectively navigate these trade-offs and identify optimal solutions along the Pareto front, an efficient multi-objective optimization strategy is required. The latent space was constructed specifically to enable continuous representation of materials, allowing the use of gradient-based optimization methods. In this context, we adopt the Multi-Gradient Descent Algorithm (MGDA), presented in [19], to perform multi-objective optimization directly within the learned latent space

7.1 Multi-Gradient Descent Algorithm

The MGDA approach allows the optimization process to account for the nature of multi-objective trade-offs by dynamically identifying descent directions that simultaneously reduce all objective functions. Instead of relying on fixed weights to balance the competing objectives, MGDA computes at each iteration a convex combination of the gradients, where the weights are determined by solving a quadratic subproblem. This ensures that the update direction either improves or maintains Pareto-stationarity, thereby guiding the solution toward regions of optimal trade-off. As the optimization progresses, the method automatically adjusts the weights, enabling a more balanced exploration of the design space without one objective systematically dominating the others. Moreover, the resulting weights provide valuable information about the relative sensitivity of each objective at the current point in latent space, offering an interpretable perspective on the optimization trajectory. This formulation makes MGDA particularly well-suited for navigating complex and conflicting objectives, such as those encountered in material selection problems involving both mechanical performance and environmental impact.

7.2 Latent Optimization Process via MGDA

MGDA reformulates the problem as finding a common descent direction in latent space that reduces all objectives simultaneously, while respecting the relative trade-offs between them. In our context, the MGDA algorithm proceeds through the following steps:

1. **Initialization**: Start at a random point in the latent space:

$$\boldsymbol{z}^{(0)} = [z_0, z_1]$$

   This 2D vector represents a potential material in the latent space learned by the VAE. Importantly, $\boldsymbol{z}$ is defined as a `torch.nn.Parameter`, which allows it to be updated during optimization using gradient descent.

2. **Objective Evaluation**: Decode $\boldsymbol{z}$ using the decoder to obtain estimated material properties. Each decoded property becomes a scalar-valued objective function:

$$\min_{\boldsymbol{z}} \{f_1(\boldsymbol{z}),\ f_2(\boldsymbol{z}),\ \ldots,\ f_k(\boldsymbol{z})\} \tag{2}$$

   In our case, $k = 5$ objectives are considered: cost, energy, waste, density-to-stiffness ratio, and yield stress. The first 4 properties will be minimized, whereas yield stress will be maximized.

3. **Gradient Computation**: Compute the gradient of each objective with respect to the latent variables $\boldsymbol{z} = [z_0, z_1]$ thanks to PyTorch's automatic differentiation, we can compute the gradient of each objective with respect to the latent coordinates, without needing explicit formulas:

$$g_i = \nabla_{\boldsymbol{z}} f_i(\boldsymbol{z}) = \begin{bmatrix} \frac{\partial f_i}{\partial z_0} \\ \frac{\partial f_i}{\partial z_1} \end{bmatrix} \tag{3}$$

   This results in k gradient vectors in R^2, one for each property being optimized.

4. **Weight Computation via Quadratic Programming**: Find a convex combination of the gradients that minimizes the norm of the weighted sum, so as to combine the gradients into a single descent direction:

$$\min_{\boldsymbol{w} \in \Delta} \left\| \sum_{i=1}^{k} w_i \nabla_{\boldsymbol{z}} f_i(\boldsymbol{z}) \right\|^2 \tag{4}$$

   subject to the simplex constraint:

$$\Delta = \left\{ \boldsymbol{w} \in R^k \;\middle|\; w_i \geq 0,\ \sum_{i=1}^{k} w_i = 1 \right\} \tag{5}$$

   This ensures that the update direction is Pareto-improving (or Pareto-stationary).

5. **Latent Vector Update**: Use the optimal weights to compute the total descent direction and update $\boldsymbol{z}$ (implemented with Stochastic Gradient Descent (SGD) Pythorch):

$$\boldsymbol{z}^{(t+1)} = \boldsymbol{z}^{(t)} - \eta \sum_{i=1}^{k} w_i^* \nabla_{\boldsymbol{z}} f_i(\boldsymbol{z}^{(t)}) \tag{6}$$

   where η is the learning rate (with a chosen value of 0.01 in the imlementation) and w_i^* are the optimal weights from the quadratic subproblem.

6. **Feasibility Enforcement**: Restrain $\boldsymbol{z}$ to stay within the learned latent space bounds:

$$\boldsymbol{z} \leftarrow \max\left(\min(\boldsymbol{z}, \boldsymbol{z}_{\max}), \boldsymbol{z}_{\min}\right)$$

7. **Iteration**: Repeat steps 2–6 for a fixed number of iterations (e.g., 500).

Note: Although $\boldsymbol{z}$ contains only two scalar components (z_0, z_1), it is continuously updated at each iteration. The decoded functions $f_i(\boldsymbol{z})$ are therefore dynamic mappings that evolve as the optimizer moves through the latent space, thanks to the power of PyTorch library [16].

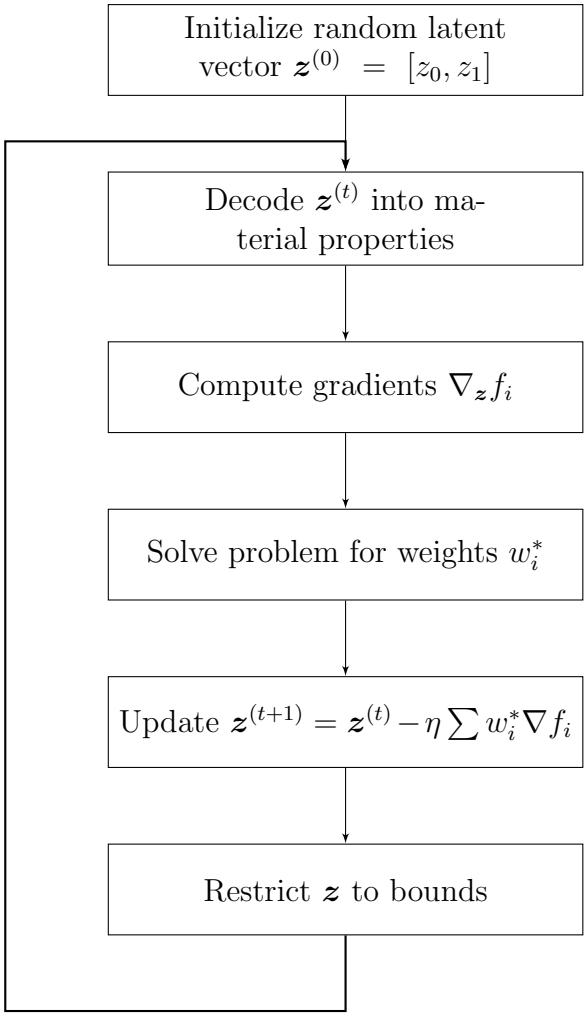

Figure 6: MGDA optimization loop for latent vector $\boldsymbol{z}$

By repeating this optimization process multiple times (e.g., 500 runs), each with different initial values of $\boldsymbol{z}$, we can obtain the Pareto front corresponding to optimal trade-offs across mechanical and environmental material properties.

7.3 Post-Optimization Material Selection

After running the optimization, we obtain a set of optimized solutions (in blue) in our latent space, as it can be observed in Figure 7. We can appreciate that they are distributed along the graph, remaining within the bounds of the latent space and located among the different pure materials.

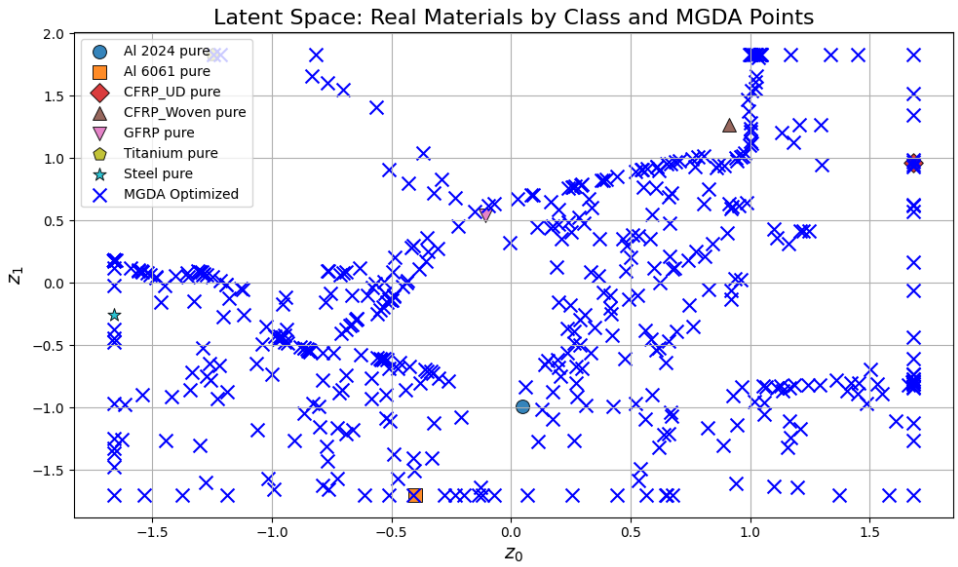

Figure 7: 2D latent space learned by the VAE colored by material class.

It was expected that the optimization process would not yield a single optimal solution, but rather a collection of optimized points, each representing the best trade-off for a given initial combination of material properties. This outcome reflects the presence of multiple local minima in the multi-objective optimization landscape. In such cases, no single solution simultaneously optimizes all objectives; instead, each solution represents a compromise between competing objectives, such as minimizing environmental impact while maximizing mechanical performance.

To make sense of this diverse set of solutions, we decode the material properties corresponding to each optimized latent vector and represent them in the form of a *Pareto front*. A Pareto front is a graphical representation of solutions in which no objective can be improved without degrading another. Each point on the front is considered *Pareto optimal*, meaning it is not dominated by any other solution. This allows us to visualize the trade-offs between conflicting properties and guide the selection of a unique point that best aligns with our design priorities.

Ultimately, one representative solution from the Pareto front will be selected for reinjection into the OpenAeroStruct (OAS) framework. This selected point can be considered as a potential material, allowing us to assess its performance and overall suitability in the structural design of the wing.

7.4 Post-Processing and Pareto Front Analysis

Upon convergence of the MGDA optimization, the decoded solutions $\hat{\zeta}$ are analyzed to visualize the trade-offs between objectives (Appendix C). Multiple Pareto fronts are constructed for different pairs of conflicting properties, revealing material candidates

that outperform existing discrete materials. This approach enables the exploration of hybrid materials that combine properties of several real-world materials, offering new opportunities for sustainable aerospace design.

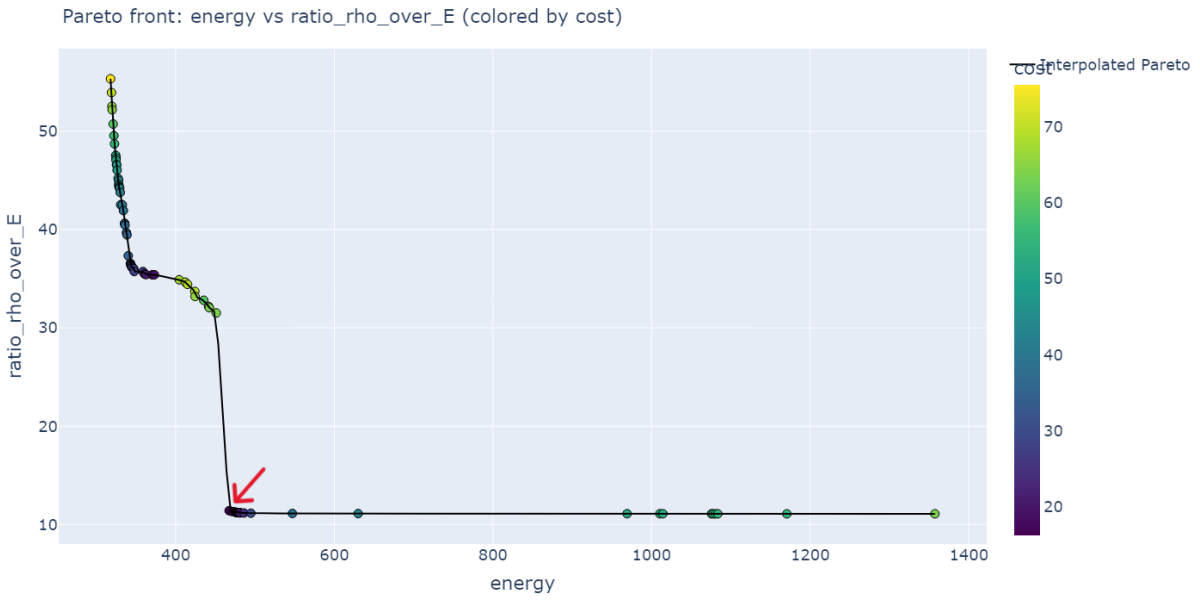

Figure 8: Pareto front obtained from multi-objective optimization in latent space.

Among the various trade-offs analyzed, the most relevant Pareto front for our study is the one that explores the density-to-stiffness ratio, with the cost scale in order to provide more information (Figure 8). This metric plays a key role in identifying material solutions that contribute to environmental performance improvements in aviation.

This graph enables the identification of a global optimum, represented by the point with the lowest density-to-stiffness ratio combined with minimal energy consumption (highlighted by the red arrow). This selected material corresponds to the following properties:

Property	**Value**	**Unit**
Energy consumption per unit mass	467.31	MJ/kg
Density-to-stiffness ratio (ρ/E)	11.40	kg/(m^3·GPa)
Effective density	1790.97	kg/m^3
Cost per unit mass	16.24	€/kg
Waste generation	0.20	kg/kg
Yield stress	1129.31	MPa
Young's modulus	157.12	GPa

Table 6: Hybrid material properties.

It may be found of interest to map the optimal point to the latent space, which can be observed in Figure 9

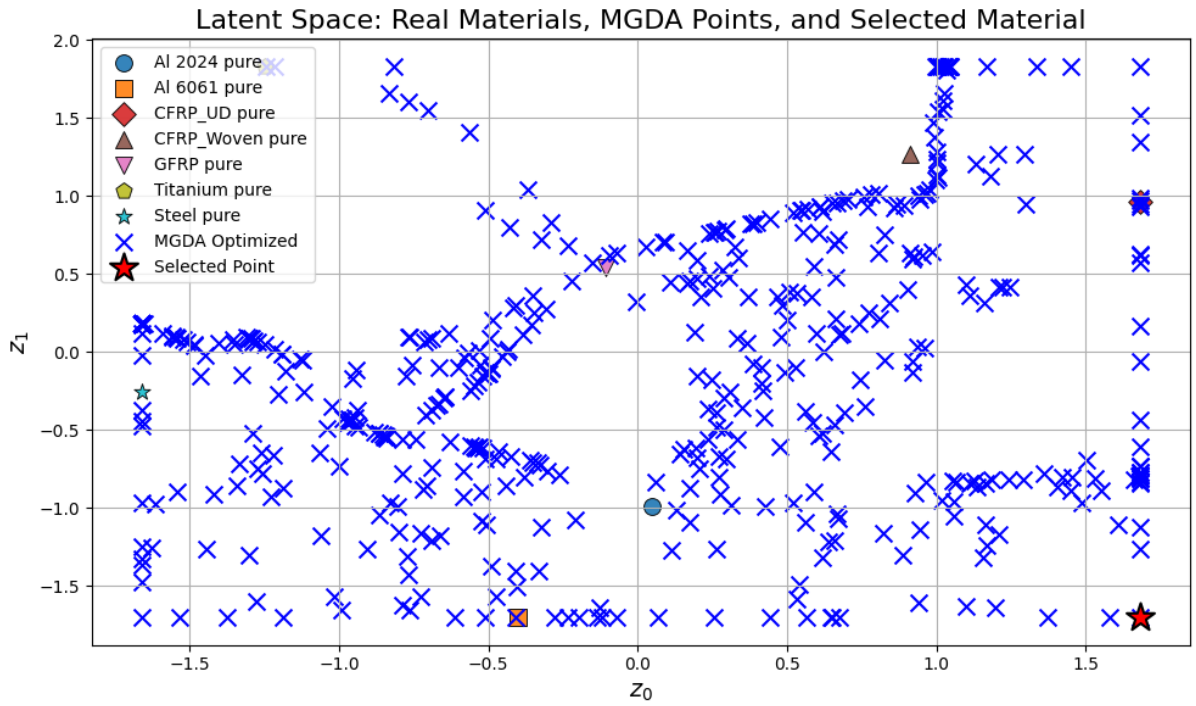

Figure 9: Pareto front obtained from multi-objective optimization in latent space.

8 OAS with Optimized Material

Building upon the initial study, we integrated a hybrid material candidate derived from the VAE-based optimization. This material is not part of the original dataset and was selected based on its favorable position in the Pareto front, offering low energy consumption and a low density-to-stiffness ratio.

The optimized material was re-injected into the OAS model to evaluate its real impact on aircraft performance and environmental metrics. As shown in Figure 10, the optimized material achieves the best trade-off: significantly lower fuel burn than traditional materials, reduced structural weight - improvement (%) presented in Table 7.

OAS Run Results:

- **Fuel consumption:** 10,149.76 kg
- **Wingbox mass:** 939.34 kg

Note: These results are optimistic since they are based on a single best-performing point identified through property interpolation by a variational autoencoder (VAE), followed by gradient-based optimization. There is currently no guarantee that a real-world material with these exact properties exists, or that such performance can be replicated in practice using a mixture of available pure materials distributed across the wingbox structure.

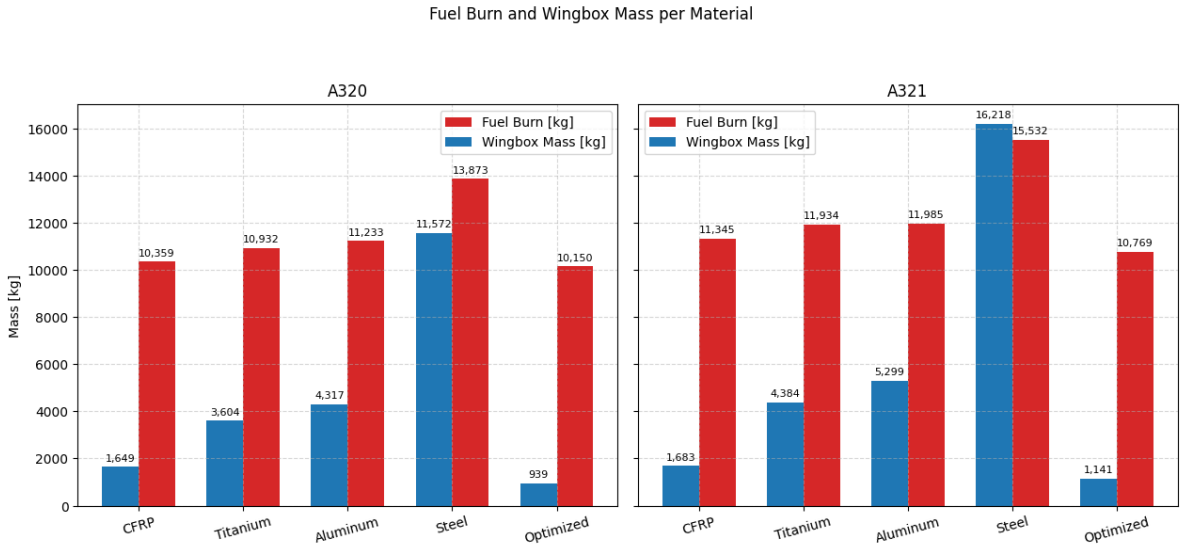

Figure 10: Fuel burn and wingbox mass per material, including the optimized material (A320 and A321).

Material	Fuel Burn Improvement [%]	Wingbox Mass Improvement [%]
CFRP	2.02	43.05
Titanium	7.16	73.94
Aluminum	9.65	78.24
Steel	26.84	91.88

Table 7: A320 Improvements of Optimized Material Compared to Pure Materials

The figures below present the environmental impact metrics (Figure 11) and the layout and aero-structural analysis of the A320 wingbox (Figure 12) for the optimized material configuration derived via the VAE-OAS methodology.

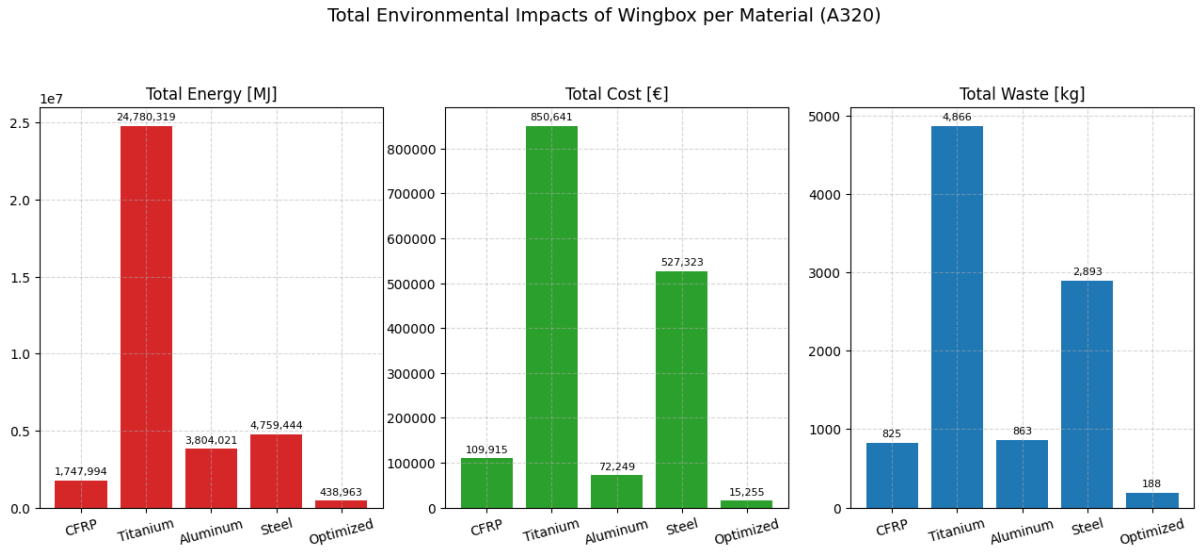

Figure 11: Environmental impact of A320 wingbox materials including the optimized solution.

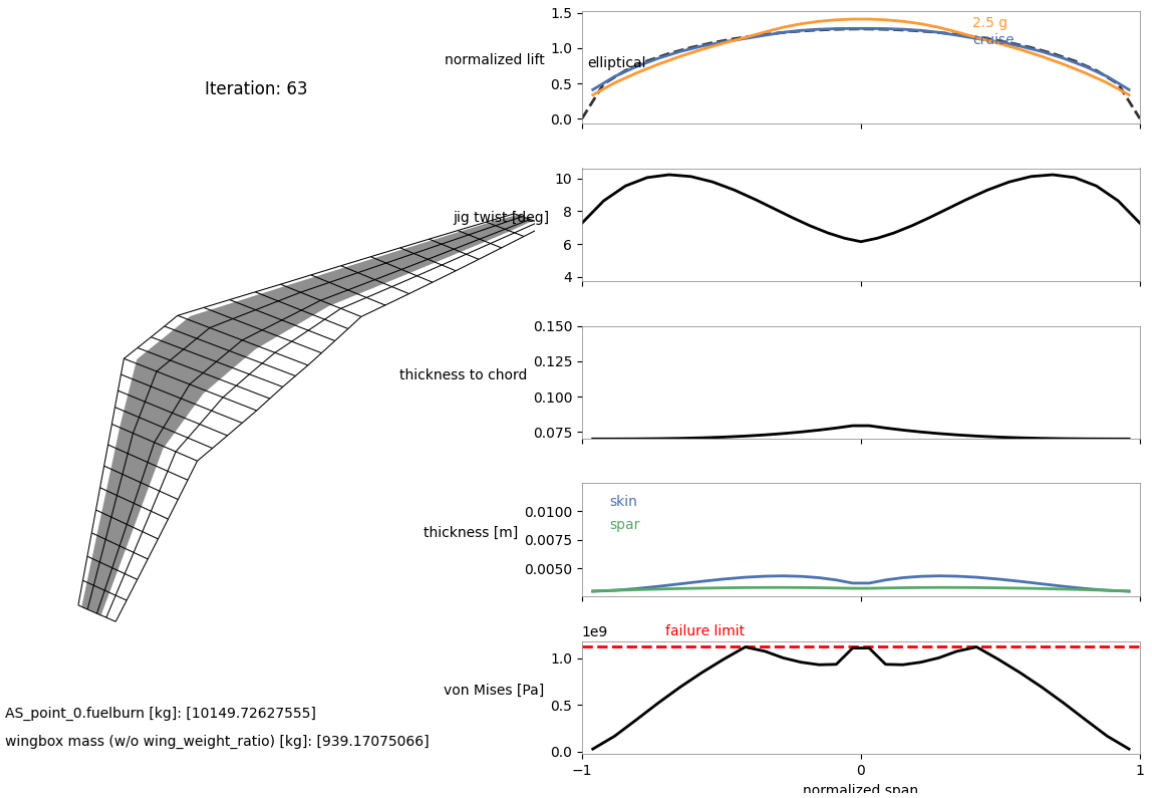

Figure 12: Wingbox plot for A320 with the optimized solution.

Again, to validate the consistency of our findings, the same analysis was applied to the A321 variant (see Annex B).

9 Conclusion and Future Work

In the first phase of this project, we focused on assessing the impact of material selection on aircraft structural and environmental performance. Using OpenAeroStruct (OAS) as the optimization backbone, we began by performing baseline optimization runs with four representative pure materials: Aluminum, CFRP, Titanium, and Steel.

To increase the resolution and realism of our analysis, we extended our material database to include the most common pure materials used in aircraft wingbox structures, specifically: Al 2024, Al 6061, CFRP-UD, CFRP-Woven, Titanium, and Steel. This data was sourced from the Granta EduPack database.

Next, we introduced a Variational Autoencoder (VAE) to learn a continuous latent representation of the discrete material property space. This enabled interpolation between materials and the generation of new candidates with hybrid properties. A multi-objective optimization procedure (MGDA) was applied in the VAE latent space to simultaneously optimize environmental and mechanical performance criteria.

The best solution from this hypothetical procedure was decoded, analyzed, and re-injected into OAS. The results showed promising improvements in fuel burn, structural weight, and environmental metrics compared to conventional materials. While these results are encouraging, it is important to note that no physical or manufacturability constraints were enforced during the optimization process. The resulting material is therefore a purely data-driven construct, not currently feasible in practice.

Looking ahead to the next semester, our objective is to bridge the gap between the idealized, data-driven material and a structurally feasible solution.

Rather than relying on a single uniform material, we plan to extend the OpenAeroStruct framework to allow for multi-material configurations. This will enable us to assign different materials to different structural components of the wingbox (such as the skin, spars, and ribs) opening the door to hybrid assemblies that can better approximate the performance of our optimized material.

By intelligently combining real materials already used in aerospace, we aim to surpass the performance of conventional configurations found in current aircraft like the A320 and A321, which are largely metallic in nature. This approach brings us closer to the design philosophy seen in newer composite-intensive aircraft such as the A350 or Boeing 787.

In parallel, we also intend to explore emerging high-performance materials from sources like the ArKema database [20]. While such materials are not yet widely used in aviation due to certification and safety constraints, they may play a key role in future aircraft structures.

By combining structural modeling, material selection, and data-driven optimization, the next phase of this project aims to move from conceptual innovation toward more practical, manufacturable, and sustainable design solutions.

A Latent Space Contour Plots

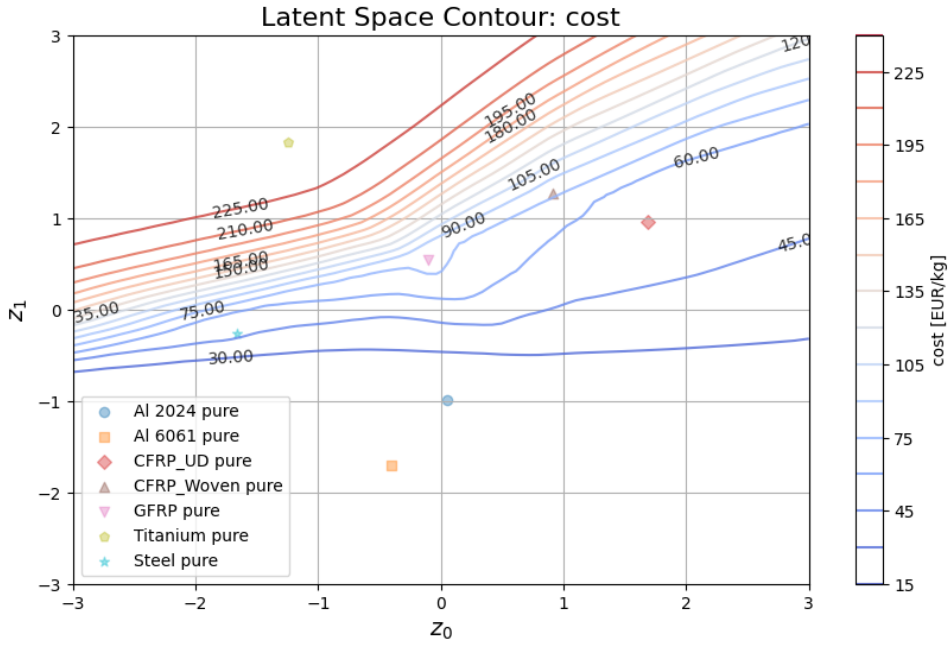

Figure 13: Latent space contour for Cost.

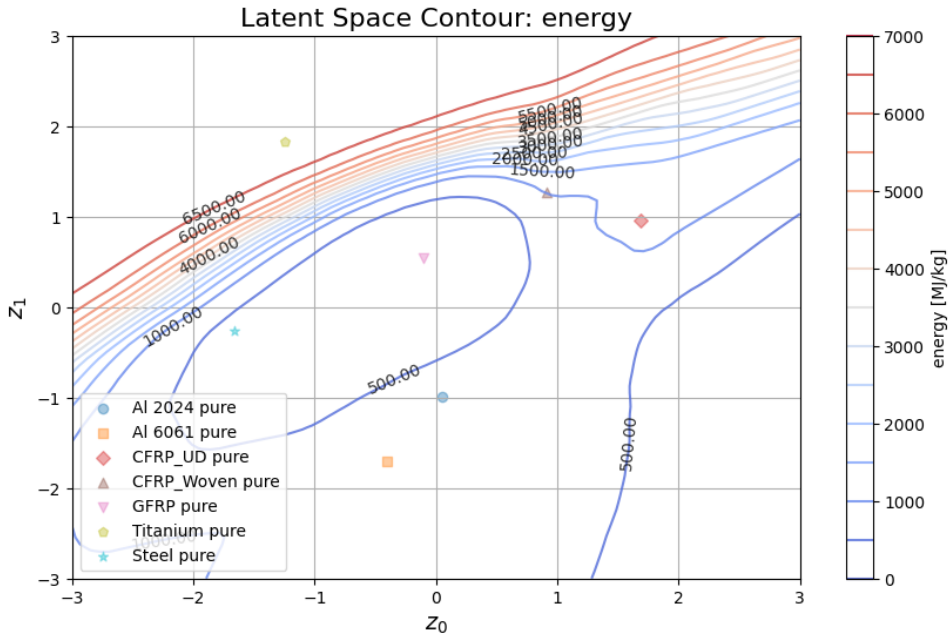

Figure 14: Latent space contour for Energy.

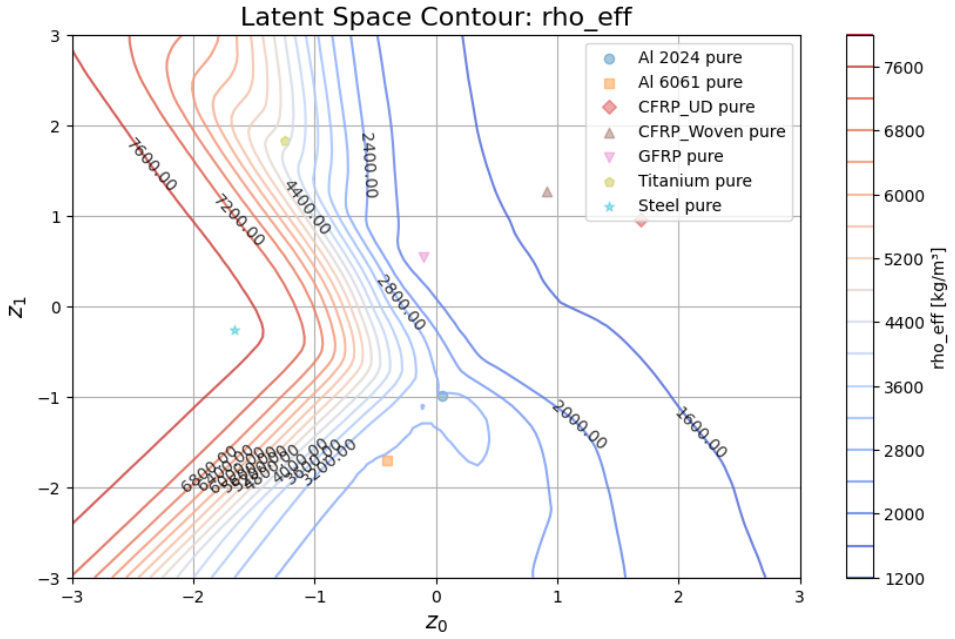

Figure 15: Latent space contour for Density.

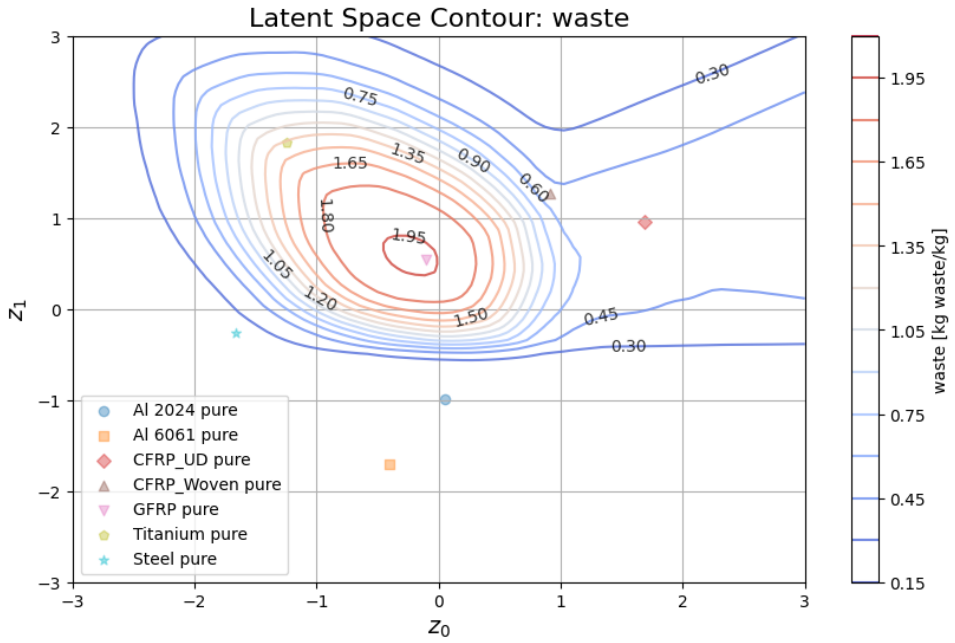

Figure 16: Latent space contour for Waste.

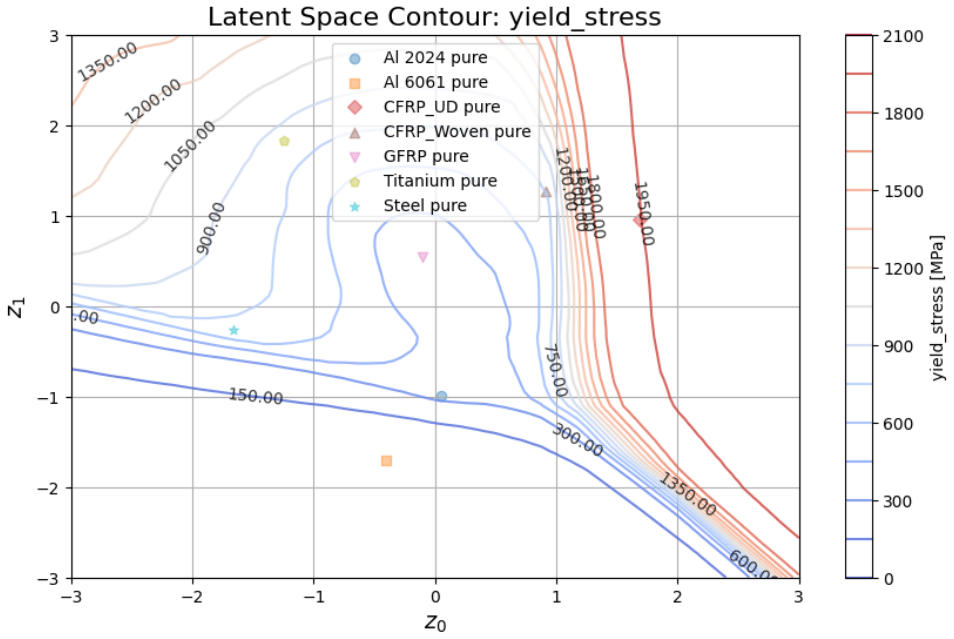

Figure 17: Latent space contour for Yield Stress.

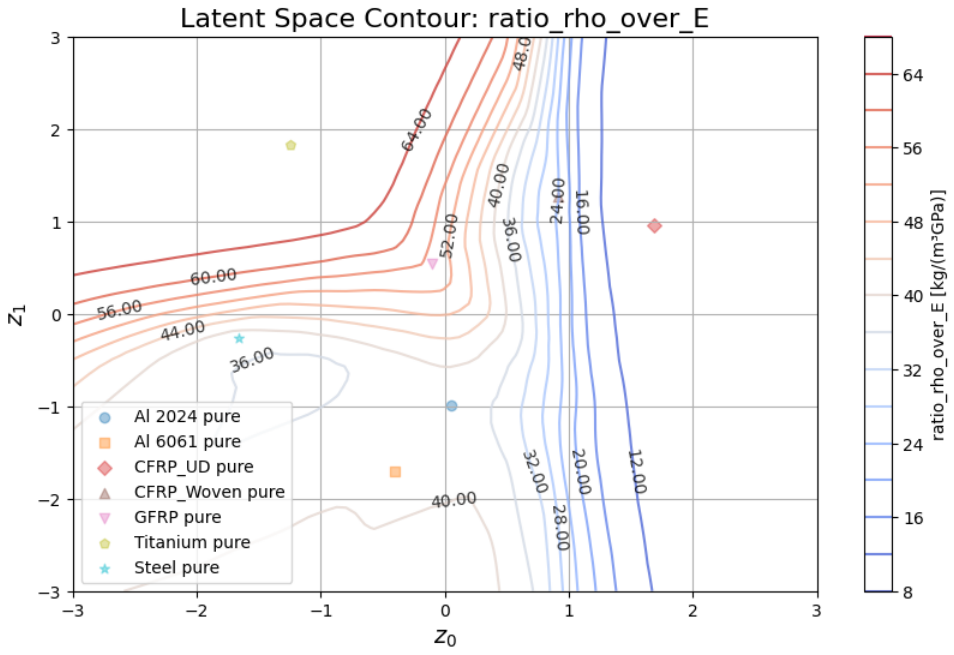

Figure 18: Latent space contour for ratio ρ over Young's Modulus.

B Environmental Impact Results for A321

As seen in Figure 19, the trend remain consistent with those observed in the A320 case.

Although absolute values are higher due to the A321's increased size, CFRP again demonstrates superior performance among the initial pure materials, while the optimized material exhibits both high efficiency and lower environmental cost compared to conventional materials.

The improvement in fuel burn and wingbox mass of the optimized material can be observed in Table 8.

Material	Fuel Burn Improvement [%]	Wingbox Mass Improvement [%]
CFRP	5.08	32.21
Titanium	9.76	73.97
Aluminum	10.15	78.47
Steel	30.67	92.96

Table 8: A321 Improvements of Optimized Material Compared to Pure Materials

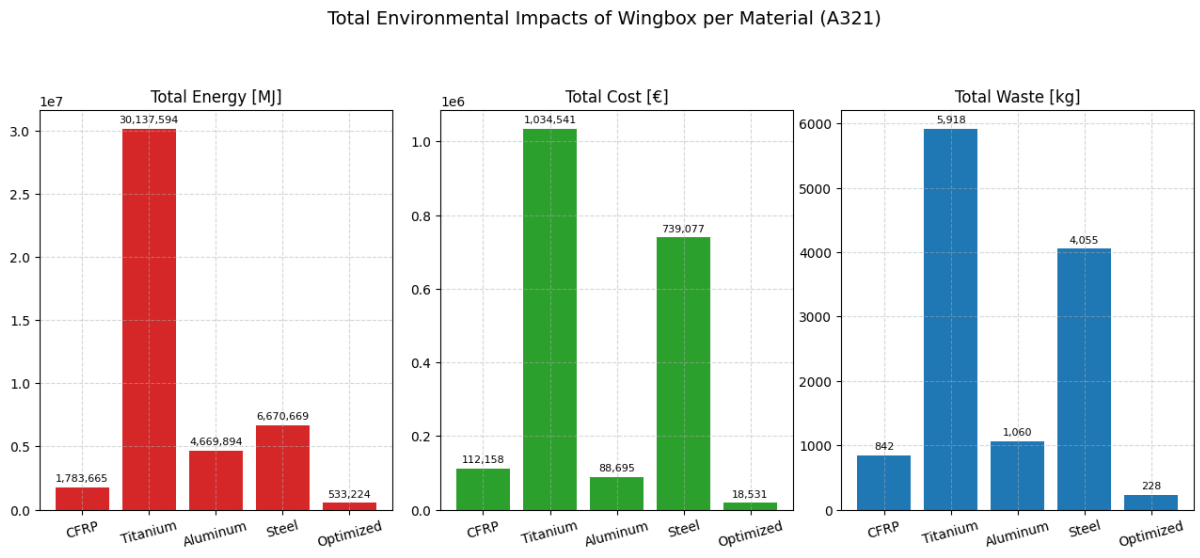

Figure 19: Environmental impact of A321 wingbox materials including the optimized solution.

Figure 20 shows the layout and aero-structural analysis of the A321 wingbox for the optimized material configuration.

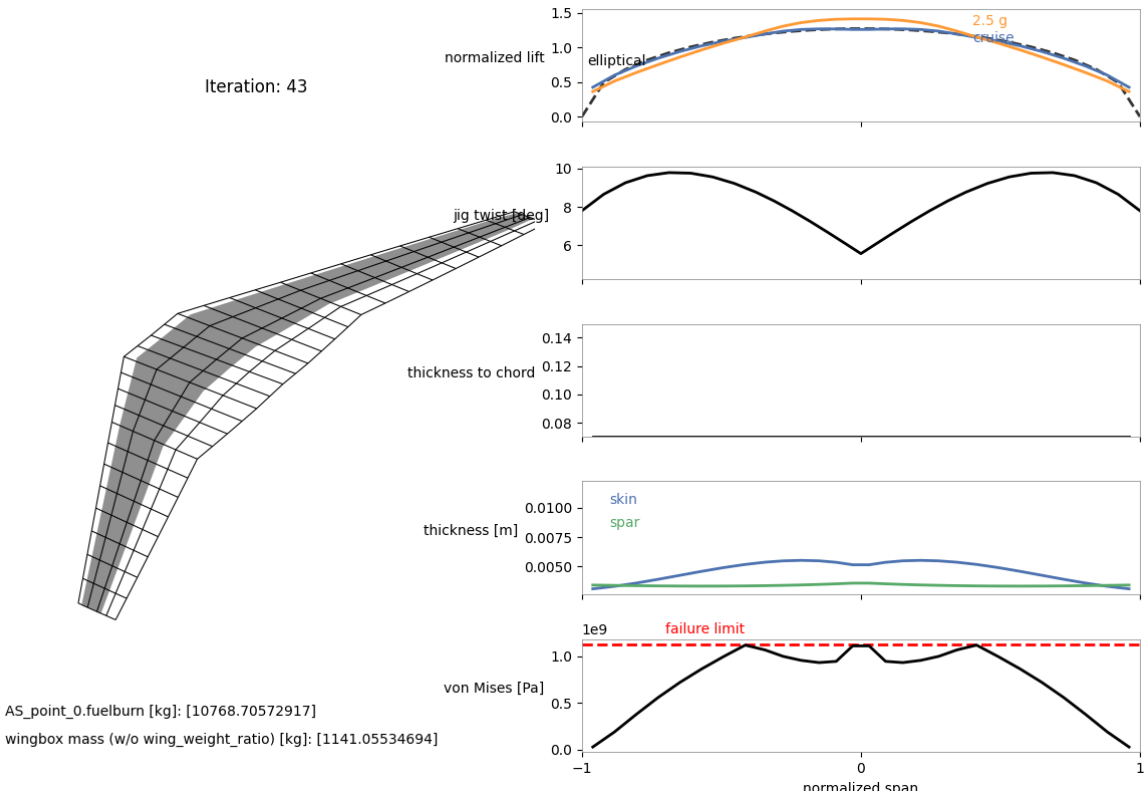

Figure 20: Wingbox plot for A321 with the optimized solution.

C Pareto fronts

Figure 21 shows a Pareto front visualization with the ratio of material density to stiffness (ρ/E) on the y-axis, expressed in kg/(m^3·GPa), material cost on the x-axis in €/kg, and color-coded by energy consumption in MJ/kg.

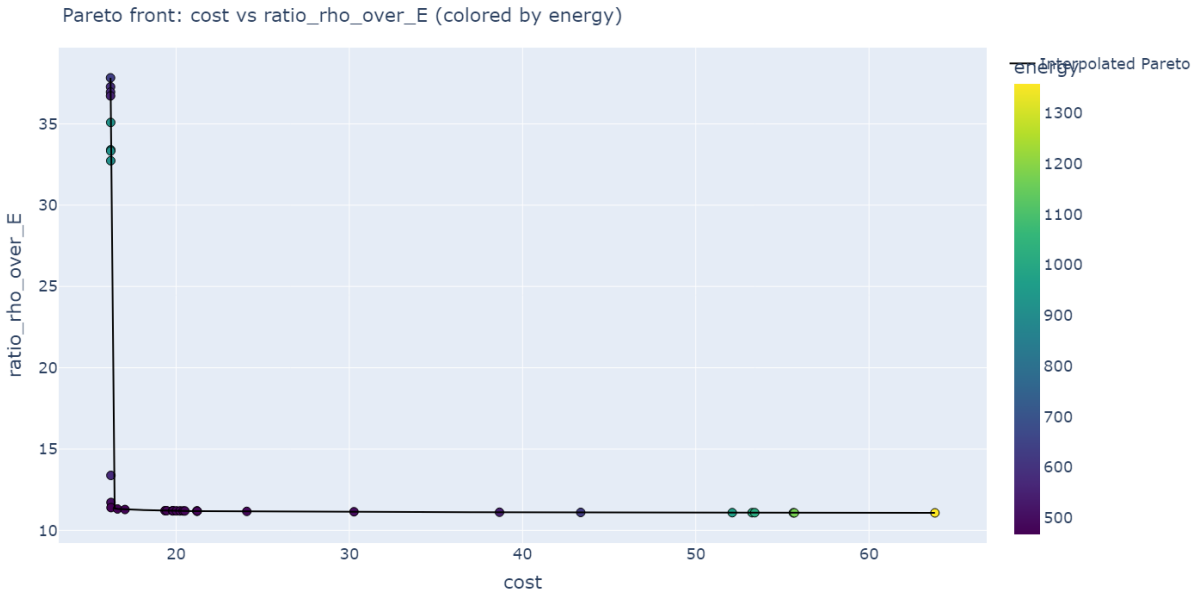

Figure 21: Pareto front (density-over-stiffness ratio vs cost) obtained from multi-objective optimization in latent space.

Figure 21 presents an alternative Pareto front view, where ρ/E remains on the y-axis [kg/(m^3·GPa)], energy consumption [MJ/kg] is on the x-axis, and color represents material cost [€/kg].

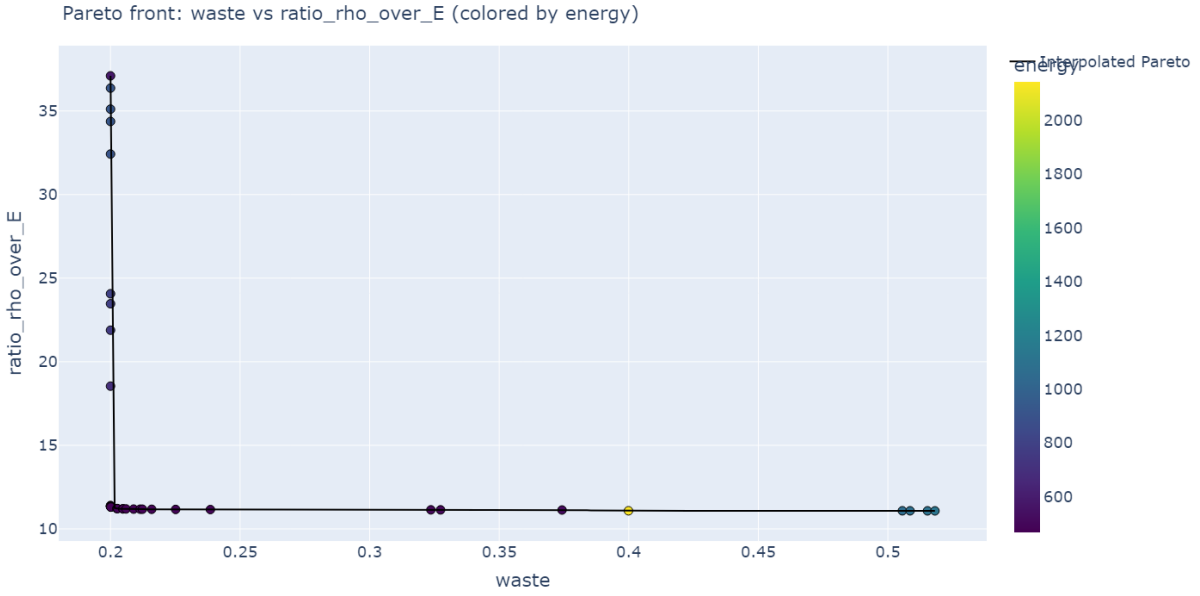

Figure 22: Pareto front (density-over-stiffness ratio vs waste) obtained from multi-objective optimization in latent space.

References

[1] P. A. Vo Dong, "Multi-objective optimization for ecodesign of aerospace cfrp waste supply chains," NNT: 2017INPT0034, Thesis, Institut National Polytechnique de Toulouse, 2017. [Online]. Available: http://oatao.univ-toulouse.fr/19911/1/VODONG_PhuongAnh.pdf.

[2] O. Boegler *et al.*, "Potential of sustainable materials in wing structural design," *Journal of Aerospace Engineering*, 2015.

[3] U. Kling *et al.*, *Future aircraft wing structures using renewable materials*. Deutsche Gesellschaft für Luft-und Raumfahrt-Lilienthal-Oberth eV, 2015.

[4] S. Waddar *et al.*, "Buckling and free vibration behavior of cenosphere/epoxy syntactic foam sandwich beam with natural fibre fabric composite facings under mechanical load," *Composites Part B: Engineering*, 2019. DOI: 10.1016/j.compositesb.2019.107133. [Online]. Available: https://doi.org/10.1016/j.compositesb.2019.107133.

[5] J. Bachmann *et al.*, "Outlook on ecologically improved composites for aviation interior and secondary structures," 2018.

[6] N. Fantuzzi *et al.*, "Mechanical analysis of a carbon fibre composite woven composite laminate for ultra-light applications in aeronautics," *Composites Part C: Open Access*, [Online]. Available: https://www.elsevier.com/locate/composites-part-c-open-access.

[7] L. Y. Llorente, J. Morlier, S. Sridhara, and K. Suresh, "A hybrid machine learning and evolutionary approach to material selection and design optimization for eco-friendly structures," *Structural and Multidisciplinary Optimization*, vol. 67, p. 69, 2024. DOI: 10.1007/s00158-024-03777-z. [Online]. Available: https://doi.org/10.1007/s00158-024-03777-z.

[8] R. Ghadge, R. Ghorpade, and S. Joshi, "Multi-disciplinary design optimization of composite structures: a review," *Composite Structures*, vol. 280, p. 114 875, 2022. DOI: 10.1016/j.compstruct.2021.114875. [Online]. Available: https://doi.org/10.1016/j.compstruct.2021.114875.

[9] S. Kilimtzidis and V. Kostopoulos, "Multidisciplinary structural optimization of novel high-aspect ratio composite aircraft wings," *Structural and Multidisciplinary Optimization*, vol. 66, p. 150, 2023, Industrial Application Paper. DOI: 10.1007/s00158-023-03600-1. [Online]. Available: https://doi.org/10.1007/s00158-023-03600-1.

[10] G. Parolin *et al.*, "A tool for aircraft eco-design based on streamlined life cycle assessment and uncertainty analysis," *Procedia CIRP*, vol. 98, pp. 565–570, 2021. DOI: 10.1016/j.procir.2021.01.152. [Online]. Available: https://www.sciencedirect.com/science/article/pii/S2212827121001827.

[11] R. P. Henderson, J. R. R. A. Martins, and R. E. Perez, "Aircraft conceptual design for optimal environmental performance," *Institute for Aerospace Studies, University of Toronto*, 2025.

[12] L. Liu, D. Kim, C. Reyner, and R. P. Liem, "Data-driven multi-range mission-based overall aircraft conceptual design optimization," 2024.

[13] MIT Department of Aeronautics and Astronautics, *Openaerostruct documentation*, Accessed: 2025-06-20, 2023. [Online]. Available: https://mdolab-openaerostruct.readthedocs-hosted.com/en/latest/.

[14] CeRAS Project, *Wing characteristics*, Accessed: 2025-03-23, 2025. [Online]. Available: https://ceras.ilr.rwth-aachen.de/tiki/tiki-index.php?page=Wing+Characteristics&structure=CeRAS.

[15] D. P. Kingma and M. Welling, "Auto-encoding variational bayes," *arXiv preprint arXiv:1312.6114*, 2013.

[16] A. Paszke *et al.*, "Pytorch: an imperative style, high-performance deep learning library," in *Advances in Neural Information Processing Systems 32 (NeurIPS 2019)*, 2019, pp. 8024–8035.

[17] J. V. O. F. Lopes, "Life cycle assessment of the airbus a330-200 aircraft," MSc Thesis, Instituto Superior Técnico, Universidade de Lisboa, Lisbon, Portugal, 2010.

[18] ANSYS Inc., *Granta EduPack Materials Database*, https://www.ansys.com/fr-fr/products/materials/granta-edupack, 2024.

[19] J.-A. Désidéri, A. Minelli, and A. Zerbinati, "A cooperative algorithm for multi-objective optimization: multiple-gradient descent algorithm (mgda)," in *4th Inverse Problems, Design and Optimization Symposium (IPDO-2013)*, Albi, France, Jun. 2013.

[20] *Arkema high performance polymers: materials database*, https://hpp.arkema.com/en/materials-database/?qc=productcomparator&step=search, Arkema, 2025.